



Synthesis of highly stable CoFe_2O_4 nanoparticles and their use as magnetically separable catalyst for Knoevenagel reaction in aqueous medium

Kula Kamal Senapati, Chandan Borgohain, Prodeep Phukan*

Department of Chemistry, Gauhati University, Gopinath Bordoloi Nagar, Guwahati 781 014, Assam, India

ARTICLE INFO

Article history:

Received 25 November 2010

Received in revised form 10 February 2011

Accepted 12 February 2011

Available online 23 February 2011

Keywords:

Cobalt ferrite

Magnetic nanoparticle

Catalyst

Magnetic separation

Knoevenagel reaction

ABSTRACT

Synthesis of spinel cobalt ferrite magnetic nanoparticles (MNPs) with average sizes in the range 40–50 nm has been achieved using a combined sonochemical and co-precipitation technique in aqueous medium without any surfactant or organic capping agent. The nanoparticles form stable dispersions in aqueous or alcoholic medium. The uncapped nanoparticles were utilized directly as a reusable catalyst for Knoevenagel reaction in aqueous ethanol (1:3). Compartmentation and recovery of the catalyst from reaction medium was done with the aid of an external magnet. High yield of corresponding Knoevenagel products were obtained within a very short time in presence of just 5 mol% of the catalyst at 50 °C.

© 2011 Elsevier B.V. All rights reserved.

1. Introduction

The use of nanoparticles as catalysts in organic transformations has attracted considerable interest in recent years, because nanoparticles provide high surface area-to-volume ratios [1,2]. Although a significant enhancement of catalytic activity can be achieved by synthesizing a catalyst in nanometer dimensions, recovery of the catalyst from the reaction mixture is a problem as they cannot be efficiently filtered out of the reaction medium. In this respect, magnetic nanoparticles hold out significant potential as a reusable catalyst because of the ease of recovery by magnetic separation which in turn prevents loss of catalyst and increases recyclability. In the recent past, functionalized magnetic nanoparticles have been utilized as efficient recoverable catalyst for various organic transformations [3–18]. Furthermore, nano-sized magnetic powders of CoFe_2O_4 are occupying an important place in the realm of synthetic and biological chemistry for their unusual properties such as multiferroic materials [19], doping or strain enhanced coercivity [20], photoinduced magnetic effects [21] and magnetic labeling of biological systems [22,23]. Much effort has therefore been undertaken to synthesize cobalt ferrite with well-defined properties which include important examples such as mechanochemical method [24], sonochemical reactions [25], co-precipitation [26–33], micro-emulsion procedure [34,35], and others [36–40]. However, in many cases, the nanoparticles

get agglomerated with non-uniform shape and cannot be stored for a long period, which is a serious disadvantage in their applications [41,42]. Sometimes, the particles formed are of poorly crystalline and high temperature annealing is required to obtain highly crystalline structure. Also, the magnetic hardening occurs only after high temperature annealing. Microemulsion methods are very effective for synthesizing nanoparticles with well-defined size and narrow size distribution, but these methods are not suitable to produce in large quantities. The most advantageous method for production of nanoparticles is coprecipitation, where particles were prepared by coprecipitating a mixture of cobalt (II) and iron(II) salts with hydroxide ions using potassium nitrate [26] or air [43] as oxidizing agent. Salazar-Alvarez and co-workers reported a convenient method for the synthesis of cobalt ferrite by aqueous coprecipitation method [29]. This method uses KNO_3 as oxidizing agent and mechanical milling is necessary in the final stage to obtain cobalt ferrite nanoparticle of desired size and shape. Moreover, the coercivity of the particle obtained by this procedure is not very high. Very recently, Kulkarni and his co-workers reported a coprecipitation method for oleic acid capped CoFe_2O_4 nanoparticles [33]. They found that, the coercivity of the CoFe_2O_4 nanoparticles is dependent on the amount of the capping agent as well as the annealing temperature. Although several reports are available in the literature for the synthesis of cobalt ferrite, most of them did not focus on the stability of the colloidal dispersions during storage. An organic capping agent such as oleic acid is necessary to make a stable colloidal dispersion of the nanoparticles.

In this report, we wish to present a simple procedure for the synthesis of highly stable spinel cobalt ferrite nanocrystals in aqueous

* Corresponding author. Tel.: +91 361 2570535; fax: +91 361 2700311.

E-mail address: pphukan@yahoo.com (P. Phukan).

ous medium without any surfactant or organic capping agent. The synthesis of the nanoparticles was achieved using aqueous co-precipitation method under repetitive ultrasonic treatment of a mixture of Co(II) and Fe(III) salt solutions. Catalytic efficiency of the as-synthesized MNPs was examined for Knoevenagel reaction [44,45] in aqueous alcohol. To the best of our knowledge this is the first report of synthesis of highly stable dispersion of nanoparticles without any stabilizing agent and direct use of MNPs for catalytic applications.

2. Experimental

2.1. Synthesis of cobalt ferrite MNPs

A combined sonochemical and co-precipitation technique was employed for the synthesis of cobalt–ferrite nanocrystals [23]. Two aqueous solutions of FeCl_3 (1.5 g, 9.3 mmol, 50 mL) and $\text{CoCl}_2 \cdot 6\text{H}_2\text{O}$ (1 g, 4.2 mmol, 50 mL) were mixed in a 200 mL flat bottom flask and placed in an ultrasonic bath. An aqueous KOH solution (3 M, 25 mL) was added dropwise under argon atmosphere with continuous ultrasonic irradiation (frequency 40 KHz and power of 40 KW). Prior to mixing, all these three solutions were sonicated for 30 min to remove dissolved oxygen. The temperature of the sonicator bath was raised up to 60 °C and the mixture was further sonicated for 30 min in air atmosphere. The black precipitate formation was observed during that time. Energy dispersive X-ray spectroscopy (EDX) analysis at this point confirms the formation of cobalt ferrite. The reaction mixture was centrifuged (14,000 rpm) at ambient temperature for 15 min. The mixture was further subjected to successive sonication (30 min) and centrifugation (15 min) for five times. The black precipitate was then separated, washed with copious amount of distilled water, ethanol and kept overnight in an incubator at 60 °C for ageing. The precipitate was further dried in oven at 100 °C for one hour and subsequently kept under high vacuum (10^{-2} bar) for 1 h. Finally, the black particles were taken in 50 mL of dry ethanol and subjected to successive sonication (30 min) and centrifugation (15 min) repeatedly till a brown colored solution appears. The precipitate was separated, dried and stored for further applications. The as synthesized cobalt ferrite particles are denoted by $\text{CoFe}_2\text{O}_4\text{-A}$.

For comparison, another batch of cobalt ferrite nanoparticles was prepared by following a procedure reported by Maaz et al. [46] in absence of capping agent. FeCl_3 (purity 99%) and $\text{CoCl}_2 \cdot 6\text{H}_2\text{O}$ (purity 99%) were taken in Co/Fe = 1:2 mole ratio and dissolved in de-ionized water. The mixture was then co-precipitated with KOH (3 M) under constant stirring maintaining the pH level of 11 and 12 and keeping the reaction temperature of 80 °C. The precipitate was washed several times and dried. Finally, the mixture was dried, and then calcined at 700 °C for 8 h. Cobalt ferrite synthesized in this way are denoted as $\text{CoFe}_2\text{O}_4\text{-B}$.

2.2. Characterization of cobalt ferrite MNPs

Formation cobalt ferrite particles was first ascertained by electron dispersive X-ray (EDX) analysis combined with scanning electron microscope (SEM). SEM was done on “LEO 1430 VP” Scanning Electron Microscope combined with Oxford EDX system (INCA X-ray microanalysis). For SEM analysis, the sample in ethanol was dispersed on aluminum foil rapped on the aluminum stub used for sample mounting. The sample was air dried and the stub was mounted in the SEM chamber. The sample was scanned at an accelerating voltage of 15 kV at a working distance of 14 mm using secondary electron detector. The particle size was measured at 300 nm resolution with magnification of 18kX.

The crystalline nature of the synthesized cobalt ferrite sample was further verified by X-ray diffraction pattern (XRD). XRD measurement of the nanoparticles was carried out on a Bruker AXS D8 using $\text{Cu K}\alpha$ radiation ($\lambda = 1.54178 \text{ \AA}$). The samples were scanned in 2θ range 10–70° at a scan rate of 5°/min.

Transmission electron microscopy (TEM) was done on a 200 kV TEM (JEOL JEM2100). Sample for TEM analysis was prepared by taking a micro drop of dilute ethanolic dispersion of the particles deposited on a carbon-coated copper grid (400 mesh size). Formation of nanocrystals was established by taking bright field TEM images at the magnifications of 25k \times and 300k \times .

The ESR spectra were recorded using a JEOL JES FA200 ESR spectrometer. Magnetic properties of the cobalt ferrite nano crystals were studied in a Lakeshore 7410 vibrating sample magnetometer (VSM). VSM measurement was done by taking 0.02 g of solid sample on the tips of the vibrating rod and analyzed at room temperature.

IR spectra were collected in the range from 400 to 4000 cm^{-1} , using Perkin Elmer Spectrum One FT-IR spectrophotometer on KBr pellets.

The specific surface area and porosity were measured by the application of Brunauer–Emmett–Teller (BET) equation and Barrett–Joyner–Halanda (BJH) method [47]. The sample was first degassed for 2 h at 200 °C and then analyzed by Backman Coulter (SA 3100) Surface Area and Pore Size Analyzer.

The thermo gravimetric analysis (TGA) measurements were made using a Netzsch STA 449 F3 Jupiter® thermo gravimetric analyzer with platinum pans. For the TGA analysis, the temperature of the system was raised to 1000 °C at a heating rate of 10 °C/min, where it was stabilized before being ramped down to room temperature at a rate of 10 °C/min.

2.3. Basicity measurement

The absorption study for evaluation of basicity of the as-synthesized sample ($\text{CoFe}_2\text{O}_4\text{-A}$) and the sample prepared by the conventional method ($\text{CoFe}_2\text{O}_4\text{-B}$) was carried out over 25 mg, 12 mg, 6 mg, 3 mg and 1 mg of each in 10 mL of 10^{-4} M chloranil solution in acetonitrile and stirred for 4 h at room temperature. The amount of chloranil adsorbed was determined from the difference in concentration of chloranil in solution before and after adsorption by using a Varian Carry 50 UV-vis spectrometer at λ_{max} of 288 nm.

2.4. Method for Knoevenagel condensation

To a solution of aldehyde (1 mmol) and ethylcyanoacetate (1 mmol, 0.12 g) in a 3 mL mixture of water and ethanol (1:3 ratio) in a round-bottom flask, was added cobalt ferrite magnetic catalyst (0.05 mmol, 0.01 g). The reaction mixture was stirred at 50 °C for appropriate time. The progress of the reaction was monitored by TLC. After completion of the reaction, the catalyst was separated with the aid of an external magnet. Ethanol was evaporated and ethyl acetate (10 mL) was added to the reaction mixture. The aqueous phase was extracted with ethyl acetate (5 mL \times 3) and the combined organic layer was dried over anhydrous Na_2SO_4 . After removing the organic solvent in a rotary evaporator, the crude product was purified by either by recrystallization (for solid compounds) or by column chromatography (liquid products) using ethyl acetate/petroleum ether as the eluant. The pure products were characterized by comparing the FT-IR (PerkinElmer, Spectrum one) and NMR (Varian 400 MHz FT-NMR) spectra with those reported in literature.

We also carried out the Knoevenagel reaction of 4-chlorobenzaldehyde and ethylcyanoacetate for 20 min and monitored the reaction for conversion, selectivity and yield by HPLC method in LCMS spectrometer (Waters Q-ToF Premier

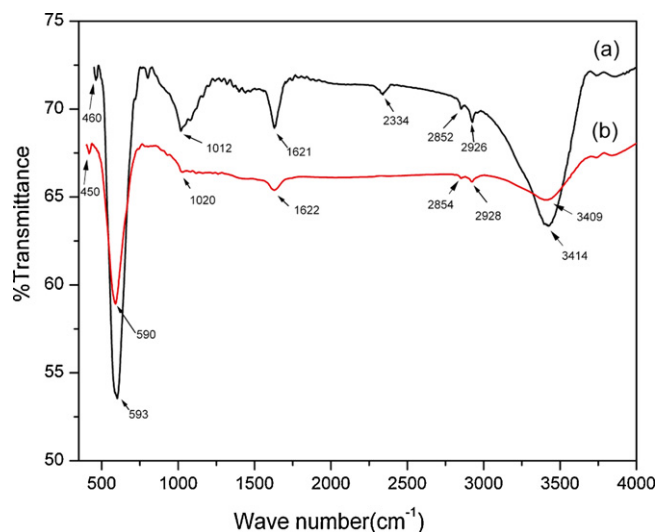


Fig. 1. IR spectra of (a) as-synthesized CoFe_2O_4 and (b) CoFe_2O_4 synthesized by normal co-precipitation method.

LC MSMS system) equipped with a TUV detector using dual wavelengths of 215 nm and 254 nm.

3. Results and discussions

3.1. Synthesis of CoFe_2O_4 nanoparticles

Cobalt ferrite nanoparticles were synthesized by means of a combined sonochemical and co-precipitation technique in aqueous medium without any surfactant or organic capping agents [23]. The synthesis was carried out in an alkaline pH under repetitive ultrasonic irradiation.

At the initial stage of the synthesis, formation of a dark brown precipitate was observed which on ultrasonication, transformed into black particles. Interestingly, the resulting black nanomaterial exhibit excellent stability. The solid nanoparticles can be easily dispersed in aqueous or alcoholic medium to form colloidal solution. Aqueous dispersion of the cobalt ferrite particles can be stored without any stabilizer for 2 months in a refrigerator. Agglomeration of the nanoparticles was not observed during storage. The morphology and properties remain unaltered during storage which is evident from electron microscopic analysis. EDX analysis confirms the desired composition of the CoFe_2O_4 nanoparticles. Formation of stable nanoparticle could be due to repetitive ultrasonic treatment during synthesis [48,49]. Cavitation effect during ultrasonic treatment might be responsible for generation of tremendous pressure and temperature [48]. This effect creates some short lived localized hot-spots which induce in situ calcinations to obtain directly cobalt ferrite particles. Hence, extra high temperature is not necessary in this method to get crystalline nanoparticles. We observed that it is essential to perform the synthesis under repetitive ultrasonic treatment. Moreover, stable dispersion does not form in aprotic solvent such as DCM due to agglomeration of the nanoparticles. Excessive hydroxyl ions entrapped in the surface of the cobalt ferrite nanocrystals during sonication [48] may be the reason of high stability in polar protic solvent and instability in less polar or non polar solvent. Due to repetitive sonication during synthesis of the catalyst, basic surface sites were formed which was further corroborated by comparing the FT-IR spectra of the as-synthesized cobalt ferrite particles and with those prepared by normal co-precipitation method (Fig. 1) [50]. The intense peak at 593 cm^{-1} in the IR spectrum is attributed to M–O tetrahedral site in the spinel structure which is more exposed in the as-synthesized sample. This

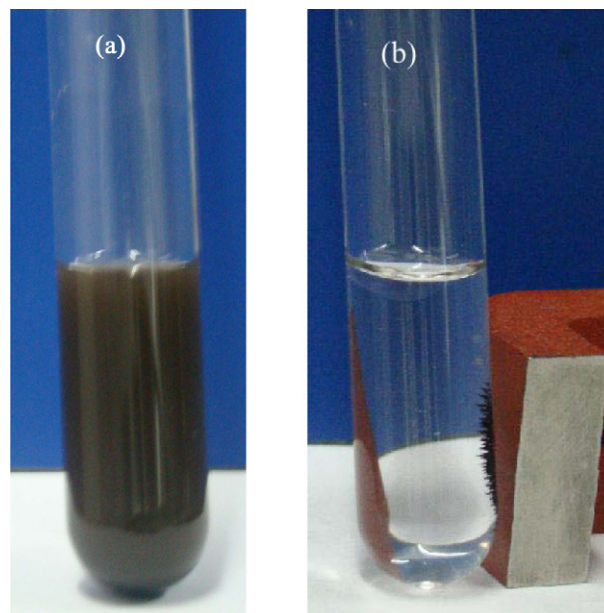


Fig. 2. (a) Dispersion in aq. ethanol (1:3) and (b) magnetic separation of CoFe_2O_4 MNPs.

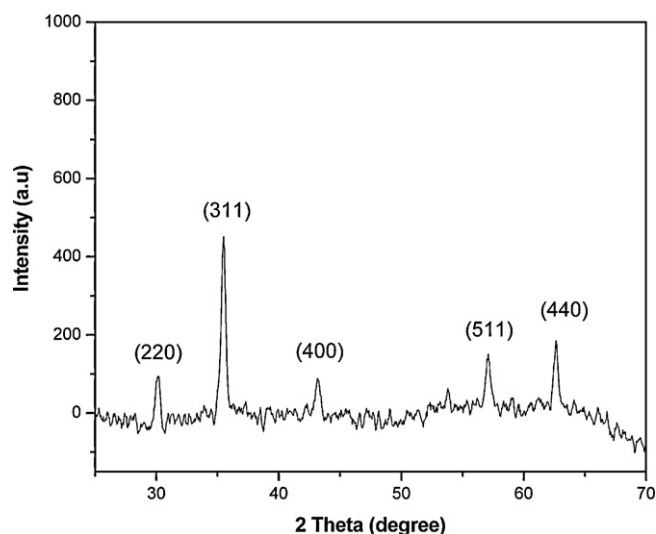


Fig. 3. XRD pattern of as-synthesized CoFe_2O_4 MNPs.

may be one of the reasons for basic nature of the as synthesized nanoparticle [51]. Moreover, the stretching frequencies for the surface adsorbed $-\text{OH}$ group are around 3400 cm^{-1} and 1620 cm^{-1} are more intense for the as-synthesized sample which indicates more polar character of the surface.

A study on the colloidal stability of as-synthesized MNPs was carried out by optical absorbance (or turbidity) measurement according to González-Caballero et al. [52]. Absorbance decay against time measured at λ_{max} of 550 nm for a period of two month at 10 days intervals revealed the stability of the nanoparticle in aqueous medium. The detail of the study is reported in supplementary information. The quasi homogeneous nanoparticle dispersion can be compartmented by using an external magnet (Fig. 2).

3.2. Structural characteristics

Fig. 3 shows the XRD pattern of the CoFe_2O_4 nanoparticles which indicates the presence of all the characteristic signals which are

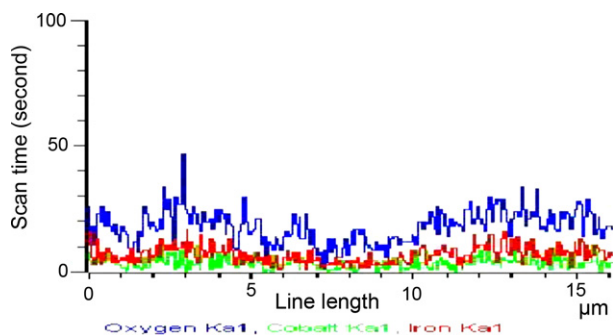


Fig. 4. Mapping analysis of CoFe_2O_4 MNPs by EDX.

present in spinel cobalt ferrite (JCPDS-International center diffraction data, PDF cards 3-864 and 22-1086) [31,53]. The crystallite size of the cobalt ferrite nanoparticles obtained from the XRD pattern using scherer's formula [54] was found to be 41 nm.

The structural composition and crystallinity of the cobalt ferrite nanoparticles was further examined by using SEM and TEM. The EDX analysis showed that the distribution of the elements (atomic percent) in the product was Co = 12.31%, Fe = 24.93%, and O = 62.76%. Thus the iron/cobalt ratio in the nanocrystals by EDX was found to be 2.02 which is very much close to the atomic ratio in the formula CoFe_2O_4 . The particle sizes were also measured in SEM micrograph and were found to be in the range of 40–50 nm.

The mapping (line scanning) analysis by EDX on as-synthesized cobalt ferrite sample (Fig. 4) revealed the uniform distribution of cobalt ferrite particles in the sample.

Fig. 5 shows the TEM image of the cobalt–ferrite nanocrystals deposited on a carbon coated copper grid. The average size of the nanoparticles from the TEM analysis was found to be 40–50 nm (Fig. 5a and b) which is consistent with the particle size obtained from XRD analysis. The diffraction pattern (SAED) obtained from the TEM (Fig. 5c) showed spinel phase CoFe_2O_4 , with the rings corresponding to reflections from the (2 2 0), (3 1 1), (4 2 2), (4 4 0) and (6 4 2) planes. The interplanar distance of the (1 1 1) reflections observed in HRTEM image (Fig. 5d) is 0.45 nm corresponds to the spinel phase crystalline nanoparticle [27].

Fig. 6 shows the N_2 adsorption–desorption isotherms of the CoFe_2O_4 MNPs. The BET surface area of the particles was found to be $48.14 \text{ m}^2/\text{g}$ as calculated by linear part of the BET plot, which is much higher than nanoparticles prepared by conventional co-precipitation method ($17.97 \text{ m}^2/\text{g}$) [50]. The total pore volume at $P/P_0 = 0.98$ is $0.20 \text{ cm}^3/\text{g}$. The BET isotherm is of type II and H3 hysteresis loop (BDDT/IUPAC classification), characteristic of mesoporous adsorbents [55].

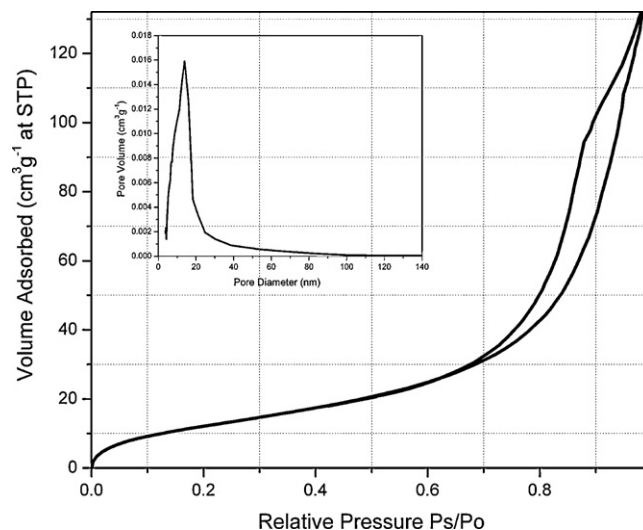


Fig. 6. BET isotherms and pore size distribution (inset) of the as-synthesized CoFe_2O_4 MNPs.

Analysis of surface basic sites on the catalyst ($\text{CoFe}_2\text{O}_4\text{-A}$) surface was carried out by following a method reported by Sugunan et al. [56] by using electron acceptors (EA) such as chloranil. For comparison, basic sites for the sample prepared by conventional co-precipitation method ($\text{CoFe}_2\text{O}_4\text{-B}$) were also estimated by using the same method. We observed a higher chloranil adsorption on the surface of ferrite $\text{CoFe}_2\text{O}_4\text{-A}$ than that of the ferrite $\text{CoFe}_2\text{O}_4\text{-B}$. The adsorption was found to be Langmuir type (shown in the supporting document) and the limiting amount of chloranil adsorbed on the reported sample ($\text{CoFe}_2\text{O}_4\text{-A}$) was found to be much higher (almost 10 times) than that of the sample conventional method ($\text{CoFe}_2\text{O}_4\text{-B}$).

We performed a comparative thermal analysis of the as synthesized magnetic particles $\text{CoFe}_2\text{O}_4\text{-A}$ and that prepared by conventional co-precipitation method ($\text{CoFe}_2\text{O}_4\text{-B}$). The TGA pattern is shown in Fig. 7 which shows that the nanoparticles undergo an initial weight loss of 5.8% and 0.5% for sample $\text{CoFe}_2\text{O}_4\text{-A}$ and $\text{CoFe}_2\text{O}_4\text{-B}$ respectively which corresponds to loss of moisture and volatile components in the sample. Thereafter a sharp decrease of 8.1% weight loss between 200°C and 400°C was observed for the $\text{CoFe}_2\text{O}_4\text{-A}$ sample which is much higher than that of the sample $\text{CoFe}_2\text{O}_4\text{-B}$ (0.6% weight loss in between 200°C and 400°C). This may be due to loss of structural water or entrapped hydroxyl groups on the surface of the sample. Further weight loss was observed (attributed to crystallization process) with a total weight loss of about 12% and 5% for sample $\text{CoFe}_2\text{O}_4\text{-A}$ and $\text{CoFe}_2\text{O}_4\text{-B}$ respectively.

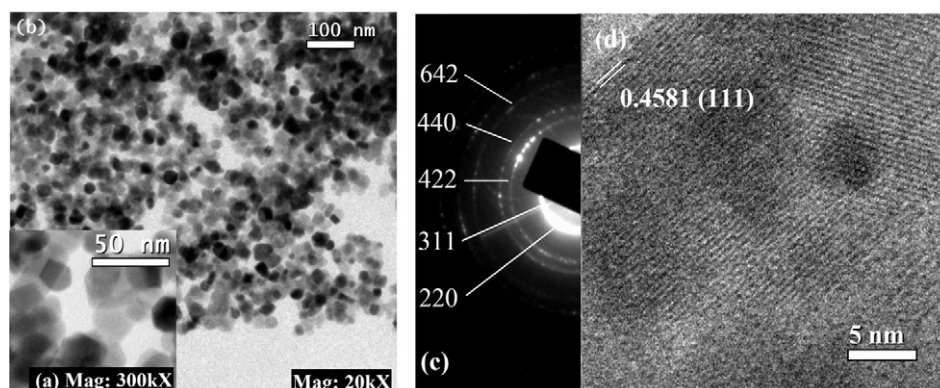


Fig. 5. TEM micrographs of the synthesized nanosized cobalt ferrite samples: (a) bright field TEM (300kX), (b) bright field TEM (20kX), (c) SAED pattern and (d) HRTEM.

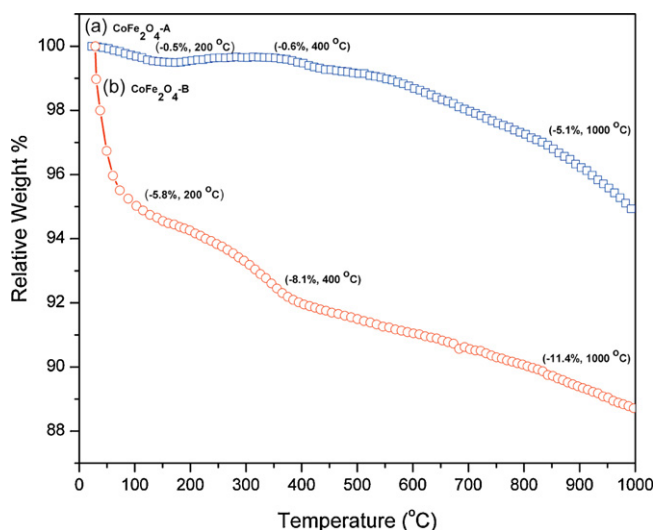


Fig. 7. TGA pattern of CoFe_2O_4 MNPs prepared by (a) ultrasonication-assisted co-precipitation method and (b) conventional method of co-precipitation.

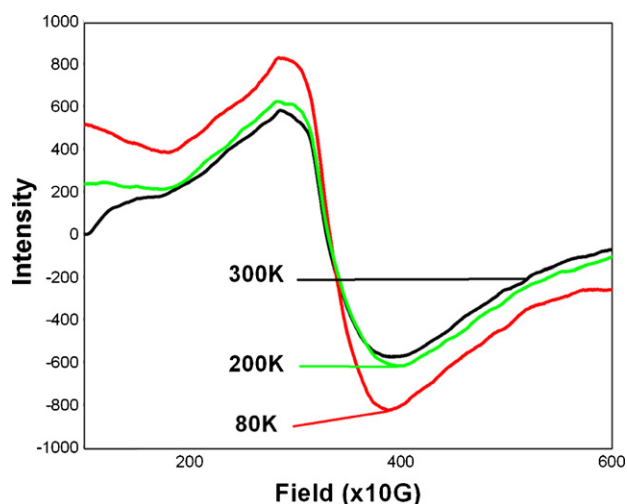


Fig. 8. ESR spectra of the cobalt ferrite sample.

3.3. Magnetic properties of the cobalt ferrite nanocrystals

The magnetic properties of the as prepared cobalt nanoparticles were investigated using ESR and VSM measurement. The ESR spectra were recorded in the temperature range from 300 K to 100 K (Fig. 8). The value of g -factor ($=2.01$) determined from EPR measurement is in good agreement with that reported in the literature for nanostructured CoFe_2O_4 particles [25]. When the spectra were recorded by varying the temperature, line broadening of the EPR signal was observed with decreasing temperature with no significant shift in resonance magnetic field, which can be attributed to strong magnetocrystalline anisotropy in the synthesized sample.

In the VSM measurement, M – H loop was taken at room temperature with a maximum applied field of ± 2 T. From the hysteresis loop both saturation magnetization (M_s) and coercivity values (H_c) were extracted. Coercivity of 2100 Oe was obtained from the extracted data where as saturation magnetization, M_s was found to be 43 emu g^{-1} . In order to understand the coercivity behavior of the cobalt ferrite nanoparticles hysteresis loops were taken at different temperatures starting from the room temperature to 80 K. Fig. 9 shows the hysteresis loops taken at three different temperatures i.e. 300 K, 200 K and 80 K. As the temperature decreased, the coer-

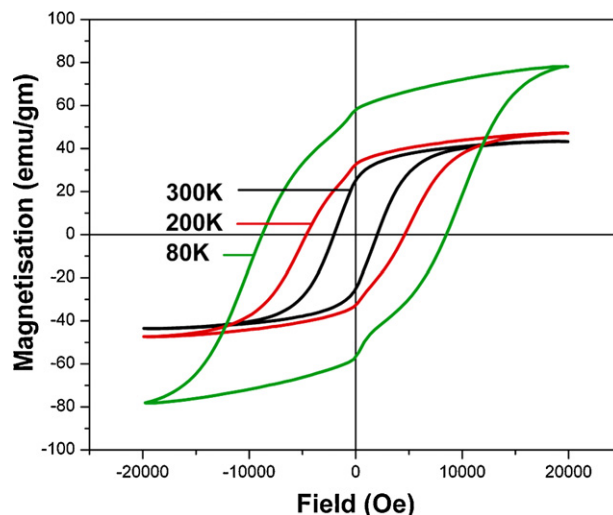


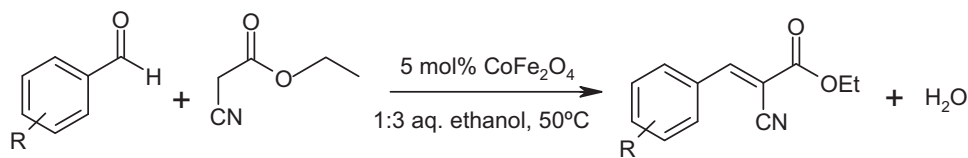
Fig. 9. Field dependence coercivity at $T = 80, 200,$ and 300 K at $\pm 2 \text{ T}$ field.

civity increased with a shoulder like feature in the M – H loop at 80 K was observed. Also the magnetization curves showed non saturation with the applied field as the temperature decreased from the room temperature. This indicates the effect of uniaxial anisotropy present in the system which causes magnetic hardening at lower temperature. The coercivity of the nanoparticles at 80 K was found to be 8.6 KOe (2.1 kOe at 300 K) with a squareness ratio (M_r/M_s) of 0.73 (0.55 at 300 K).

3.4. Catalytic activity

The Knoevenagel reaction is a popular and widely used synthetic pathway for carbon–carbon formation reaction in organic synthesis [44,45]. There are also few recent reports on the use of heterogeneous catalysts for Knoevenagel reaction [57–59]. However, the use of magnetic nanoparticles is advantageous as compared to other heterogeneous catalytic methods. Functionalized magnetic nanoparticles were also used by few researchers for Knoevenagel reaction [11–14]. Jones has shown that functionalized magnetic nanoparticles works better than silica functionalized catalyst for Knoevenagel reaction [11]. However, prior functionalization of nanoparticles for introduction of basic site is necessary for catalytic applications [11–14]. Our method has the advantage that no further modification of the magnetic particles is necessary for utilization as catalyst. We observed that the pH of the 0.02 molar solution of the as-synthesized CoFe_2O_4 MNPs is 8.98 at 25°C . Hence, we presumed that these cobalt ferrite nanoparticles can directly be used as catalyst for Knoevenagel condensation between different aromatic aldehydes and ethylcyanoacetate (Scheme 1).

Since, water is the most desired solvent from the point of green chemistry and the catalyst forms a homogeneous aqueous dispersions, we initially, carried out the reaction in water as solvent at room temperature. The test reaction was carried out by taking 4-chlorobenzaldehyde and ethylcyanoacetate as the model substrate and the progress of the reaction was monitored by TLC. In all cases, the product was isolated for determination of actual product yield. Initial reaction at room temperature produced low yield of the product after 3 h of reaction. However, at 50°C , the reaction produced 72% of isolated product yield after 1 h of reaction. Thereafter, we have examined the reaction using different solvent to find out the optimum reaction condition. The influence of solvent on the Knoevenagel reaction between *p*-chloro benzaldehyde and ethylcyanoacetate was investigated at 50°C and the products were isolated after 1 h of reaction. Results were presented in Fig. 10.



Scheme 1. Knoevenagel condensation reaction.

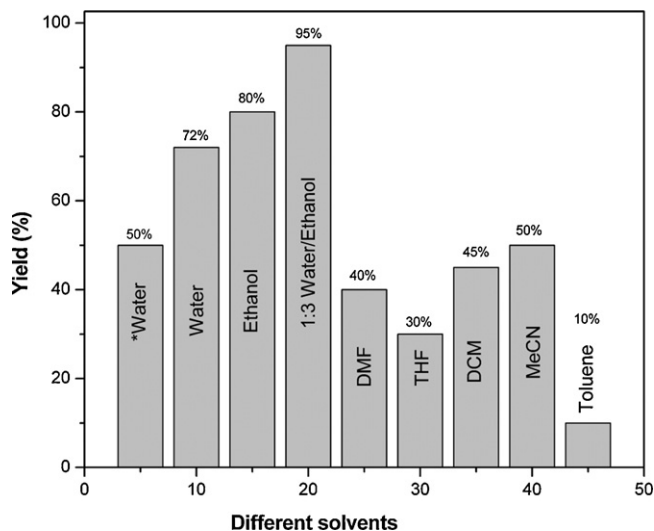
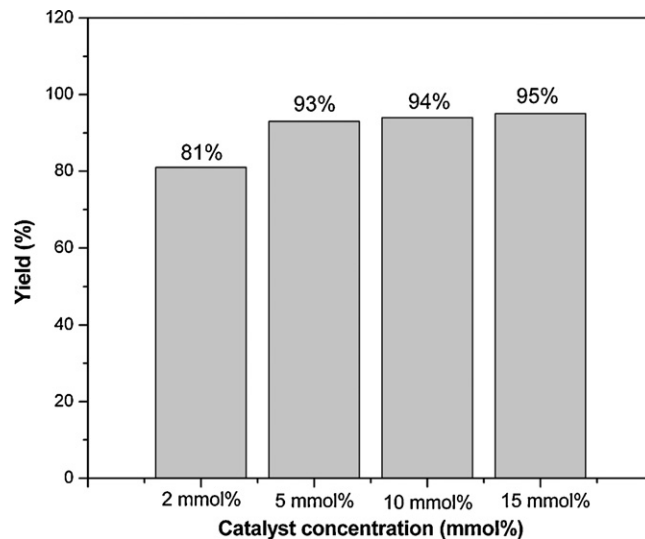


Fig. 10. Solvent effect on Knoevenagel condensation using 5 mol% of cobaltferrite nanocrystals at 50 °C (*water, at 25 °C).

We observed that a polar protic solvent such as ethanol is very effective for achieving good product yield. However, in water the yield is lower than in ethanol due to low solubility of the reactants. It is well known that, if the charge species are involved as in case of Knoevenagel reaction, the transition-state is better solvated by polar solvents in homogeneous phase, decreasing the activation free enthalpy and enhancing rate and hence increase the product yield. When the reaction was carried out in 1:3 water–ethanol mixture, we obtained 95% isolated yield of the corresponding product. Repetition of the reaction revealed that the reaction is very fast in aqueous ethanol and it takes only 25 min for completion of reaction. However use of other solvents such as DMF, THF, DCM, MeCN and toluene did not produce good results. Low yield in polar aprotic solvent is may be due to poor stability of the colloidal dispersion of the MNPs in these solvents. High dispersability of the MNPs in water and ethanol makes the system a quasi-homogenous phase which facilitate a better interaction of the nanoparticle with the reactants and hence a faster reaction rate. This is in good agreement with previous observations in the homogenous phase [60] for high reaction rate and high product yield. In non polar solvent such as toluene, the product yield is very low which is in accordance with the polar mechanism involved in the reaction as well as non-dispersibility of the magnetic nano catalyst in this solvent. Hence, high activity of the reaction in polar solvents was observed. Finally, aqueous ethanol (1:3) was found to be the solvent of choice for the reaction. The quasi homogeneous nanoparticle dispersion can be compartmented by using an external magnet.

For comparison, a reaction of *p*-chlorobenzaldehyde and ethylcyanoacetate was performed using the CoFe_2O_4 MNPs prepared by conventional method ($\text{CoFe}_2\text{O}_4\text{-B}$) keeping all the reaction conditions same. We observed that the reaction in this case is very slow and 53% of the corresponding product was formed after 6 h of reaction.

Fig. 11. Effect of CoFe_2O_4 MNP concentration on the Knoevenagel reaction using 1:3 water ethanol solvent.

The reaction was further examined in presence of different amount of catalyst. The yield generally increased with the increasing concentration of the catalyst from 2 mol% to 5 mol%. However, further increase of the molar concentration of the catalyst from 5 to 15 mol% did not significantly increase the yield of the product (Fig. 11). Hence, a concentration of 5 mol% of the MNPs was chosen for the optimum yield of Knoevenagel products.

After optimizing the reaction conditions we extended the procedure using different aldehydes, the results are summarized in Table 1.

Reactions were carried out using 1 mmol of aldehyde, 1 mmol of ethylcyanoacetate and 0.05 mmol of cobalt ferrite in a 3 mL of a mix-

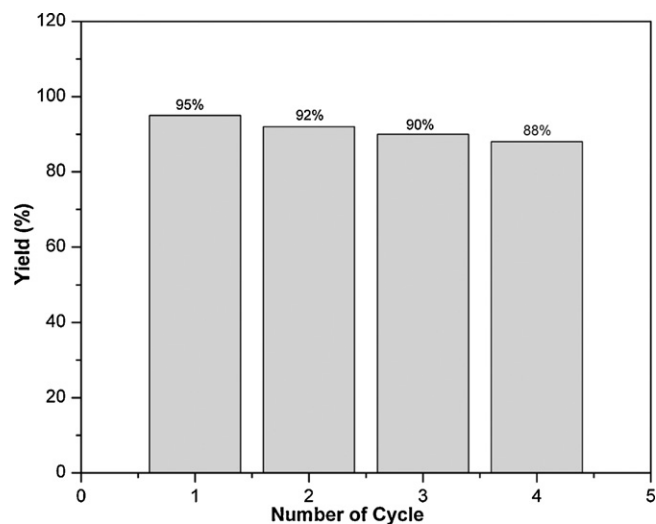
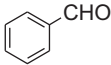
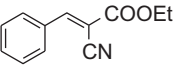
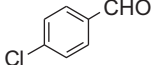
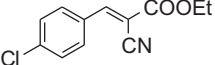
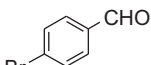
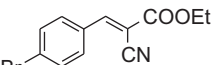
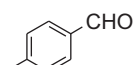
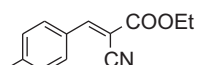
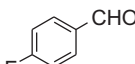
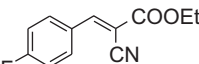
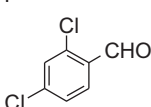
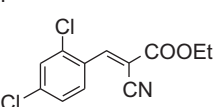
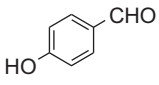
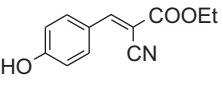
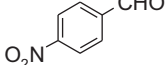
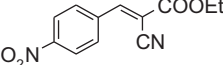
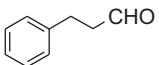
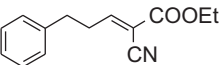
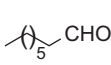
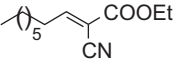
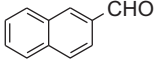
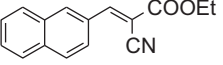
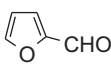
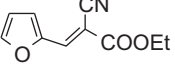
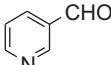
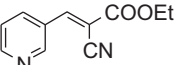
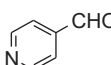
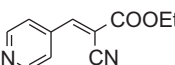


Fig. 12. Recyclability for Knoevenagel reaction of 4-chlorobenzaldehyde and ethylcyanoacetate.

Table 1
Knoevenagel condensation with different aldehydes catalyzed by CoFe₂O₄ magnetic nanocatalyst^a.

Entry	Aldehydes	Product	t (min)	Yield (%) ^b
1			20	93
2			20	95
3			15	96
4			10	90
5			10	96
6			10	94
7			10	87
8			2	96
9			30	70
10			30	68
11			30	96
12			15	87
13			10	89
14			20	94

^a Reaction condition: aldehyde, 1 mmol; ethyl cyanoacetate, 1 mmol; CoFe₂O₄ MNPs, 5 mol% solvent (1:3 water/ethanol), 3 mL; temp. 50 °C.

^b Isolated yield.

ture (1:3) of water and ethanol. The reaction mixture was stirred using a magnetic stirring bar at 50 °C for the appropriate time as indicated by TLC. After completion of the reaction, MNPs were separated by an external magnet and after usual work up the crude product was purified either by recrystallization or column chromatography. The products were characterized by comparing the IR and NMR spectroscopic data which revealed the excellent purity. High catalytic activity of the un-capped cobalt ferrite nanocrystals for Knoevenagel reaction may be primarily due to surface basicity of the MNPs.

As expected for nucleophilic addition reactions, aromatic aldehydes with electron-withdrawing group such as nitro (–NO₂) moiety were more reactive, with 96% yield being achieved (entry 8), while much lower isolated yield was obtained for the reaction of aldehydes containing an electron-donating group such as hydroxyl (–OH) (entry 7). This trend in product yield is consistent with the fact that in case of electron withdrawing groups, the possibility of attack of the carbanion at the carbonyl carbon is enhanced compared to that of the electron withdrawing groups. The hetero-

cyclic aldehydes (entry 11–14) also afforded good to excellent yield. For the reaction of aliphatic aldehyde, the short chain aldehyde was found to be slightly more reactive than long chain aldehyde (entries 9 and 10). Thereafter we examined the reaction of 4-chlorobenzaldehyde with ethyl cyanoacetate in 10 mmol scale. The reaction produced 94% of isolated yield after 20 min of reaction.

3.5. Recyclability of the catalyst

The recyclability of the catalyst was checked by carrying out repeated runs on the same batch of the used 5 mol% cobalt ferrite magnetic catalyst in Knoevenagel condensation of 4-chlorobenzaldehyde and ethylcyanoacetate (Fig. 12). Catalytic activity of the cobalt ferrite did not decrease significantly even after four catalytic cycles. The SEM and XRD analysis of the nanoparticle revealed that the morphology of the recovered MNPs remains unaltered during the recycling process which indicates that the catalyst is stable towards oxidation during the reaction.

4. Conclusions

In conclusion, a new type of CoFe_2O_4 magnetic nanocatalyst has been developed with average sizes in the range 40–50 nm using a combined sonochemical and co-precipitation process. The resulting nanocrystals, as well as its dispersion exhibit excellent stability in ethanol or aqueous solvent and can be stored without any stabilizer for months. Agglomeration of the uncapped nanoparticles was not observed during storage. The as-synthesized nanoparticles showed high values of coercivity, saturation magnetization and squareness ratio. These MNPs were used as efficient quasi-homogenous catalyst for Knoevenagel condensation reaction of several aldehydes with ethylcyanoacetate in mild conditions. Catalyst could be recovered from the reaction mixture by compartmentation with the aid of an external magnet and could be re-used four times without significant loss in activity.

Acknowledgements

Financial support from DST (India) (grant no. SR/S1/RPFC-07/2006) is gratefully acknowledged. We thank IIT Guwahati for analytical facilities.

Appendix A. Supplementary data

Supplementary data associated with this article can be found, in the online version, at doi:10.1016/j.molcata.2011.02.007.

References

- [1] D. Astruc, F. Lu, J.R. Aranzas, *Angew. Chem. Int. Ed.* 44 (2005) 7852.
- [2] M.T. Reetz, M. Maase, *Adv. Mater.* 11 (1999) 773.
- [3] M. Kawamura, K. Sato, *Chem. Commun.* (2006) 4718.
- [4] J. Liu, X. Peng, W. Sun, Y. Zhao, C. Xia, *Org. Lett.* 10 (2008) 3933.
- [5] N.T.S. Phan, C.S. Gill, J.V. Nguyen, Z.J. Zhang, C.W. Jones, *Angew. Chem. Int. Ed.* 45 (2006) 2209.
- [6] D. Guin, B. Baruwati, S.V. Manorama, *Org. Lett.* 9 (2007) 1419.
- [7] P.D. Stevens, G. Li, J. Fan, M. Yen, Y. Gao, *Chem. Commun.* (2005) 4435.
- [8] G. Evans, I.V. Kozhevnikov, E.F. Kozhevnikova, J.B. Claridge, R. Vaidyanathan, C. Dickinson, C.D. Wood, A.I. Cooper, M.J. Rosseinsky, *J. Mater. Chem.* 18 (2008) 5518.
- [9] V. Polshettiwar, B. Baruwati, R.S. Varma, *Chem. Commun.* (2009) 1837.
- [10] L. Aschwanden, B. Panella, P. Rossbach, B. Keller, A. Baiker, *ChemCatChem* 1 (2009) 111.
- [11] N.T.S. Phan, C.W. Jones, *J. Mol. Catal. A: Chem.* 253 (2006) 123.
- [12] Y. Zhang, Y. Zhao, C. Xia, *J. Mol. Catal. A: Chem.* 306 (2009) 107.
- [13] Y. Zhang, C. Xia, *Appl. Catal. A: Gen.* 366 (2009) 141.
- [14] C.S. Gill, W. Long, C.W. Jones, *Catal. Lett.* 131 (2009) 425.
- [15] J. Li, Y. Zhang, D. Han, Q. Gao, C. Li, *J. Mol. Catal. A: Chem.* 298 (2009) 31.
- [16] A. Schätz, M. Hager, O. Reiser, *Adv. Funct. Mater.* 19 (2009) 2109.
- [17] V. Polshettiwar, R.S. Varma, *Tetrahedron* 66 (2010) 1091.
- [18] K.V.S. Ranganath, J. Kloesges, A. Schäfer, F. Glorius, *Angew. Chem. Int. Ed.* 49 (2010) 7786.
- [19] H. Zheng, J. Wang, S.E. Lofland, Z. Mohaddes-Ardabili, L. Ma, T. Zhao, L. Salamanca-Riba, S.R. Shinde, S.B. Ogale, F. Bai, D. Viehland, Y. Jia, D.G. Schlom, M. Wuttig, A. Roytburd, R. Ramesh, *Science* 303 (2004) 661.
- [20] J. Ding, Y.J. Chen, Y. Shi, S. Wang, *Appl. Phys. Lett.* 77 (2000) 3621.
- [21] K.E. Giri, M. Kirkpatrick, P. Moongkhamklang, S.A. Majetich, V.G. Harris, *Appl. Phys. Lett.* 80 (2002) 2341.
- [22] M. Platt, G. Muthukrishnan, W.O. Hancock, M.E. Williams, *J. Am. Chem. Soc.* 127 (2005) 15686.
- [23] C. Borgohain, K.K. Senapati, D. Mishra, K.C. Sarma, P. Phukan, *Nanoscale* 2 (2010) 2250.
- [24] H. Yang, X. Zhang, A. Tang, G. Oiu, *Chem. Lett.* 33 (2004) 826.
- [25] K.V.P.M. Shafi, A. Gedanken, *Chem. Mater.* 10 (1998) 3445.
- [26] H. Tamura, E. Matijevic, *J. Colloid Interface Sci.* 90 (1982) 100.
- [27] Y.I. Kim, D. Kim, S.C. Lee, *Phys. B: Condens. Matter.* 42 (2003) 337.
- [28] F. Bensebaa, F. Zavaliche, P.L. Ecuery, R.W. Cochrane, T. Veres, *J. Colloid Interface Sci.* 227 (2004) 104.
- [29] R.T. Olsson, G. Salazar-Alvarez, M.S. Hedenqvist, U.W. Gedde, F. Lindberg, S.J. Savage, *Chem. Mater.* 17 (2005) 5109.
- [30] S. Bhattacharyya, J.-P. Salvétat, R. Fleurier, A. Husmann, T. Cacciaguerra, M.-L. Saboungi, *Chem. Commun.* (2005) 4818.
- [31] X. Cao, L. Gu, *Nanotechnology* 16 (2005) 180.
- [32] S. Sun, H. Zeng, D.B. Robinson, S. Raoux, P.M. Rice, S.X. Wang, G. Li, *J. Am. Chem. Soc.* 126 (2004) 273.
- [33] M.V. Limaye, S.B. Singh, S.K. Date, D. Kothari, V.R. Reddy, A. Gupta, V. Sathe, R.J. Choudhary, S.K. Kulkarni, *J. Phys. Chem. B* 113 (2009) 9070.
- [34] N. Moumen, M.P. Pileni, *Chem. Mater.* 8 (1996) 1128.
- [35] C. Liu, A.J. Rondinone, Z. Zhang, *Pure Appl. Chem.* 72 (2000) 37.
- [36] E. Manova, B. Kunev, D. Paneva, I. Mitov, L. Petrov, C. Estournes, C. D'Orléans, J.-H. Rehspringer, M. Kurmoo, *Chem. Mater.* 16 (2004) 5689.
- [37] T. Meron, Y. Rosenberg, Y. Lareah, G. Markovich, *J. Magn. Magn. Mater.* 292 (2005) 11.
- [38] E. Tirosh, G. Shemer, G. Markovich, *Chem. Mater.* 18 (2006) 465.
- [39] T. Hyeon, Y. Chung, J. Park, S.S. Lee, Y.-W. Kim, B.H. Park, *J. Phys. Chem. B* 106 (2002) 6831.
- [40] A. Franco Júnior, E.C. de Oliveira Lima, M.A. Novak, P.R. Wells Jr., *J. Magn. Magn. Mater.* 308 (2007) 198.
- [41] T. Prozorov, R. Prozorov, Y. Koltypin, I. Felner, A. Gedanken, *J. Phys. Chem. B* 102 (1998) 10165.
- [42] A.J. Rondinone, S.C.S. Anna, Z.J. Zhang, *J. Phys. Chem. B* 103 (1999) 6876.
- [43] M. Kiyama, *Bull. Chem. Soc. Jpn.* 51 (1978) 134.
- [44] E. Knoevenagel, *Berichte* 31 (1898) 2585.
- [45] G. Jones, *Org. React.* 15 (1967) 204.
- [46] K. Maaza, A. Mumtaza, S.K. Hasanaina, A. CeylanK, *J. Magn. Magn. Mater.* 308 (2007) 198.
- [47] S.J. Greg, K.S.W. Sing, *Adsorption, Surface Area and Porosity*, Academic, New York, 1997.
- [48] T.J. Merson, *Sonochemistry: The Uses of Ultrasound in Chemistry*, Royal Society of Chemistry, Cambridge, 1990.
- [49] W. Chen, W. Cai, Y. Lei, L.A. Zhang, *Mater. Lett.* 50 (2001) 53.
- [50] Z. Jiao, X. Geng, M. Wu, Y. Jiang, B. Zhao, *J. Colloids Surf. A* 313 (2008) 31.
- [51] C.G. Ramankutty, S. Sugunan, *Appl. Catal. A: Gen.* 218 (2001) 39.
- [52] J. de Vicente, A.V. Delgado, R.C. Plaza, J.D.G. Durán, F. González-Caballero, *Langmuir* 16 (2000) 7954.
- [53] T. Hyeon, Y. Chung, J. Park, S. Lee, Y.-W. Kim, B.H. Park, *J. Phys. Chem. B* 106 (2002) 6831.
- [54] B.D. Cullity, *Elements of X-ray Diffraction*, Addison Wesley, London, 1959, 261.
- [55] J.B. Silva, W. de Brito, N.D.S. Mohallem, *Mater. Sci. Eng. B* 112 (2004) 182.
- [56] S. Sugunan, K.B. Sherly, G.D. Rani, *React. Kinet. Catal. Lett.* 51 (1993) 525.
- [57] V.S.R. Rajasekhar Pullabhotla, A. Rahman, S.B. Jonnalagadda, *Catal. Commun.* 10 (2009) 365.
- [58] J.M. Khurana, K. Vij, *Catal. Lett.* 138 (2010) 104.
- [59] A. Kumar, M. Dewan, A. Saxena, A. De, S. Mozumdar, *Catal. Commun.* 11 (2010) 679.
- [60] I. Rodriguez, G. Sastre, A. Corma, S. Iborra, *J. Catal.* 183 (1999) 14.